

ZERO-MASS PULSATILE JETS FOR UNMANNED UNDERWATER VEHICLE MANEUVERING

K. Mohseni*

Research and Engineering Center for Unmanned Vehicles,
Department of Aerospace Engineering Sciences,
University of Colorado at Boulder, CO 80309-0429,

ABSTRACT

Compact zero-mass pulsatile jet actuators are proposed for low speed maneuvering, ducking, and station keeping of small underwater vehicles. To this end, optimization of synthetic jets for maximal thrust generation is investigated. Flow field of such jets are initially dominated by vortex ring formation. Pinched-off vortices characterize the extremum impulse accumulated by the leading vortex ring in a vortex ring formation process. Relevant parameters in this process are identified to design simple and low cost zero-mass pulsatile jet actuators. Prototypes of such actuators are built for underwater maneuvering and propulsion. The actuators could be used in two ways: (i) to improve the low speed maneuvering and station keeping capabilities of traditional propeller driven underwater vehicles, (ii) and as a synthetic jet for flow control and drag reduction at higher cruising speeds.

INTRODUCTION

Unmanned Underwater Vehicles (UUVs) will play a major role in the future environmental control and monitoring, underwater archeology, search and rescue missions, maintenance/monitoring of underwater structures, and underwater battlespace. Two main categories of unmanned underwater vehicles are autonomous underwater vehicles (AUVs) and remotely operated vehicles (ROVs). AUVs operate for relatively long periods underwater without direct human guidance while ROVs are powered and teleoperated via a tether connected to a surface command ship.

AUVs are attractive in these areas for a number of reasons. Because of their size and their nonreliance on human operators, AUVs are often less expensive

to operate than remotely operated or manned underwater vehicles. ROVs partially share the same advantages. However, ROV's operating range can be limited significantly by the requirement of a physical connection between the ROV and a host ship or platform. Furthermore, the required tether can be fouled in restricted environments such as kelp forests or under ice [1].

Most AUV designs (e.g. WHOI's REMUS, MIT's Odyssey, and Florida Atlantic University's new modular AUV Morpheus) have traditionally been based on a propeller thruster combined with control fins (or shrouded thrusters) to propel and steer the vehicle. Such designs are often streamlined (torpedo-like body shape) and optimized for low drag during forward motion. Maneuvering control forces are generated by lift or deflection forces created by fluid flow over the control surfaces. At cruising speeds, and for relatively uncluttered spaces, this paradigm is extremely efficient and effective. However, at low speeds and in tight spaces the magnitude of the available control forces drops significantly. Consequently, such vehicles are difficult to dock. As a result much current effort is devoted to the development of docking mechanisms.

ROVs, which are not designed for cruising, typically follow the so-called "Box Design" or a multipointon design. Better low speed maneuvering and control are achieved by sacrificing the low drag body-of-revolution design and adding multiple thrusters at different locations and directions. MBARI's Tiburon and WHOI's JASON [2] are among successful ROV designs in this category. Successful AUV designs in this category include WHOI's ABE [3] and SeaBED and Stanford's OTTER [4]. While Propellers are excellent when they work at constant speed they will be less efficient for small motion corrections when the motions of propellers involve less than a full shaft rotation. This results in degraded control precision and possibly periodic oscillations of the vehicle's position.

Recovery of AUVs is a challenging problem. Vari-

*Assistant Professor, AIAA Member,
mohseni@colorado.edu

Copyright © 2004 by the author. Published by the American Institute of Aeronautics and Astronautics, Inc. with permission.

ous techniques have been suggested in the literature. For example, Odyssey II, an underwater robot developed by the Massachusetts Institute of Technology (MIT) Sea Grant College Program, relies on homing and uses a commercially available ultra-short baseline (USBL) acoustic system to guide Odyssey II into a capture net [1]. A single aft-mounted thruster and four control planes mounted on the aft portion of the fuselage are used to control the vehicle. Since the vehicle does not have any lateral and vertical thrusters, forward motion is required for maneuvering. Minimum maneuvering speed is found to be approximately 0.5 m/sec and turn radius is approximately 5 m.

In summary, underwater maneuvering (especially at low speeds) and docking procedures represent a major challenge in the design of AUVs and ROVs. To this end, experimental platforms for testing, evaluating, and developing a low speed maneuvering (LSM) capability for UUVs are recently developed at the University of Colorado [5; 6]. A compact zero-mass pulsatile jet technology is proposed that could overcome many of the shortcomings described above for low speed maneuvering of AUVs and ROVs, and enable new types of lower cost micro-AUVs. As described below, *this propulsion scheme has no protruding components that increase drag, has very few moving parts, and takes up relatively little volume.* Such hybrid designs which incorporate both a main propeller and a distributed set of pulsatile jets will improve low speed AUV performance. While propellers clearly perform best at cruising speeds, pulsatile jets can significantly augment low speed maneuverability, and enable occasional loitering/hovering actions.

PULSATILE JET PROPULSION

The propulsion scheme suggested here is loosely inspired by the propulsion of cephalopods (e.g. squid and octopi), salp, and jellyfish [7; 8; 9; 10; 11; 12]. Squid (see Figure 1) use a combination of fin undulations and a jet which can direct thrust at any angle through a hemisphere below the body plane. Their complete range of locomotory behavior rivals that of reef fish. Jet propulsion swimming of the squid is accomplished by drawing water into the mantle cavity, and then contracting the mantle muscles to force water out through the funnel. The funnel, which is directly behind and slightly below the head, can be maneuvered so as to direct jets in a wide range of directions. Another example of pulsatile jet locomotion is jellyfish swimming [13], which relies upon

repeated contractions of an umbrella-shaped structure, or bell. During contraction, circular subumbrellar muscles pull the sides of the bell inward, reducing the volume of the subumbrellar cavity, and forcing water out through the velar aperture. Water is drawn back into the subumbrellar cavity during the relaxation phase. The jellyfish can optimize its propulsion by controlling the diameter, velocity, and profile at the exit of the velar aperture.

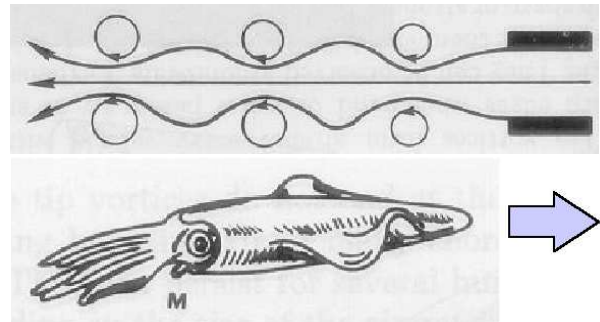


Figure 1: Squid locomotion by pulsed jet.

Weihhs [12], Seikman [10], and recently Krueger and Gharib [14] have shown that a pulsed jet can give rise to a greater average thrust force than a steady jet of equivalent mass flow rate. In a pulsed jet, an ejected mass of fluid rolls into a toroidal vortex ring which moves away from its source. A continuously pulsatile jet, therefore, produces a row of vortex rings (see Figure 1). At high pulsing frequency, the jet structure can become increasingly turbulent.

Vortex ring jets can be generated using a variety of mechanical devices. While a squid generates vortex rings by muscle contraction around the mantle, one of the simplest ways to generate vortex rings and pulsatile jets in the laboratory is the motion of a piston pushing a column of fluid through an orifice; the so-called cylinder-piston mechanism (see Figure 2). This system provides a simplified approximation to natural pulsatile jet generation, and it is amenable to experimental, computational, and analytic study. When the piston pushes fluid through the cylinder,

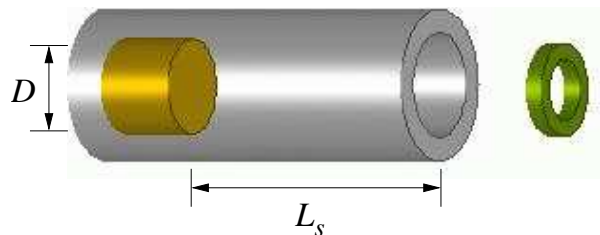


Figure 2: Cylinder piston mechanism.

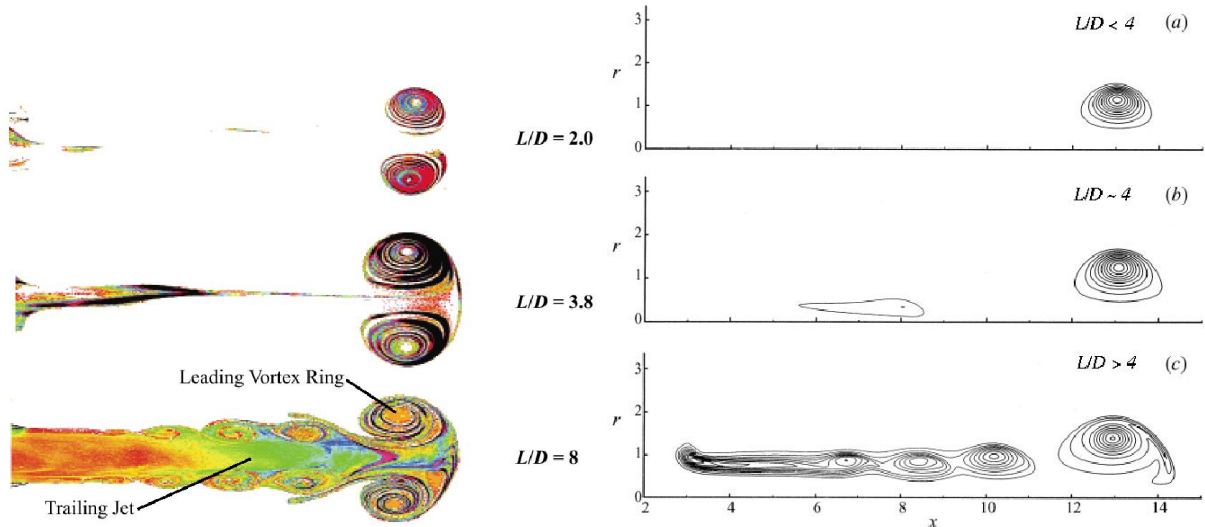


Figure 3: **Left:** Experimentally obtained fluid vorticity profiles during the vortex ring pinch-off process (for various L/D formation numbers) [15]. **Right:** Numerical simulation of vortex ring formation at various formation numbers [16]. Only one half of the symmetric jet cross section is presented.

the boundary layer of the fluid expelled from the cylinder will separate and roll up into a vortex ring at the orifice edge. Experiments [15] have shown that for large enough ratios (above 4) of piston stroke versus diameter (L/D), the generated flow consists of a leading vortex ring followed by a trailing jet. See Figure 3(a) for experimental results, and Figure 3(b) for corresponding numerical simulations.

It was both experimentally [15] and analytically [17] observed that the limiting stroke L/D occurs when the generating apparatus is no longer able to deliver energy, circulation and impulse at a rate comparable with the requirement that a steadily translating vortex ring has maximum energy with respect to kinematically allowable perturbations. Mohseni and Gharib [17] suggest that the properties of the leading vortex ring are the final outcome of a relaxation process, dependent only on the first few integrals of the motion (the energy, E , impulse, I , and circulation, Γ). Mohseni [18] argued that the energy extremization in Kelvin’s variational principle has a close connection with the entropy maximization in statistical equilibrium theories. Numerical evidence for a relaxation process in axisymmetric flows to an equilibrium state has been provided by Mohseni *et al.* [16] in a direct numerical simulation of the vortex ring pinch-off process. Similar phenomena are observed in the alternating vortex shedding behind bluff bodies [19].

In squid and jellyfish, the exit diameter of the

cylinder (mantle or bell) varies during the expulsion of fluid. This technique optimizes propulsive output. We have recently shown that a time varying shear layer velocity mechanism can also manipulate pulsatile jet behavior (see [16; 17]). While the mechanisms here are even more complicated than the piston-cylinder model, this model does provide useful guidance on the overall physical phenomena at work.

SYNTHETIC JET ACTUATOR (SJA) PROTOTYPES

While the piston-cylinder model is attractive for theoretical studies and ease of experimental set-up, there are more practical means to generate pulsatile jets. In the synthetic jet concept (Figure), the inward movement of a diaphragm draws fluid into a chamber. The subsequent outward diaphragm movement expels the fluid, forming a vortex ring or a jet depending on the formation number. Repetition of this cycle results in a pulsatile jet. Because of the asymmetry of the flow during the inflow and outflow phases, a net fluid impulse is generated in each cycle, even though there is no net mass flow through the chamber over one cycle. To this end, prototypes of pulsatile jet generators using the Helmholtz cavity concept are designed and built at the University of Colorado. Various actuation techniques can be employed for actuating the diaphragm. These includes, but not limited to, using solenoid plungers, acoustic speakers, electrostatic and piezoelectric actuation.

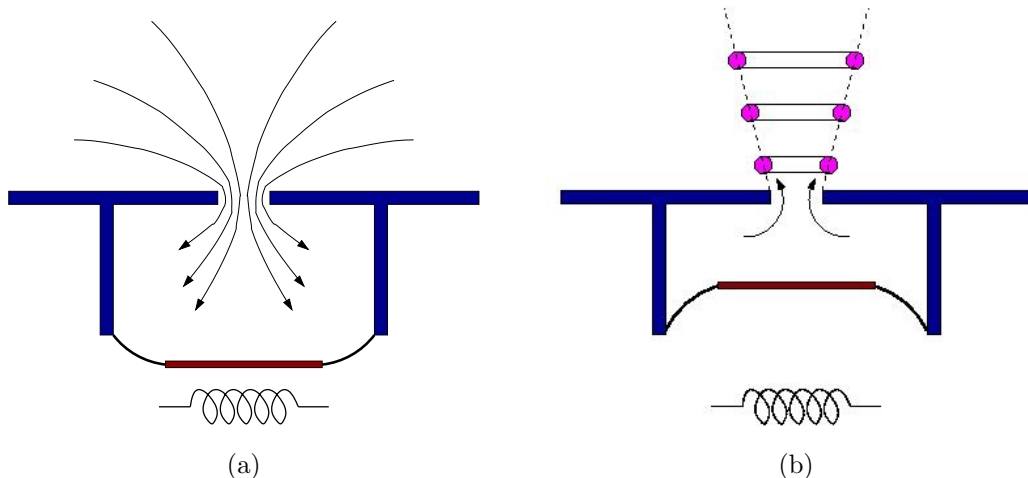


Figure 4: Synthetic jet actuator concept: (a) Fluid entrainment; (b) Vortex ring formation during fluid ejection.

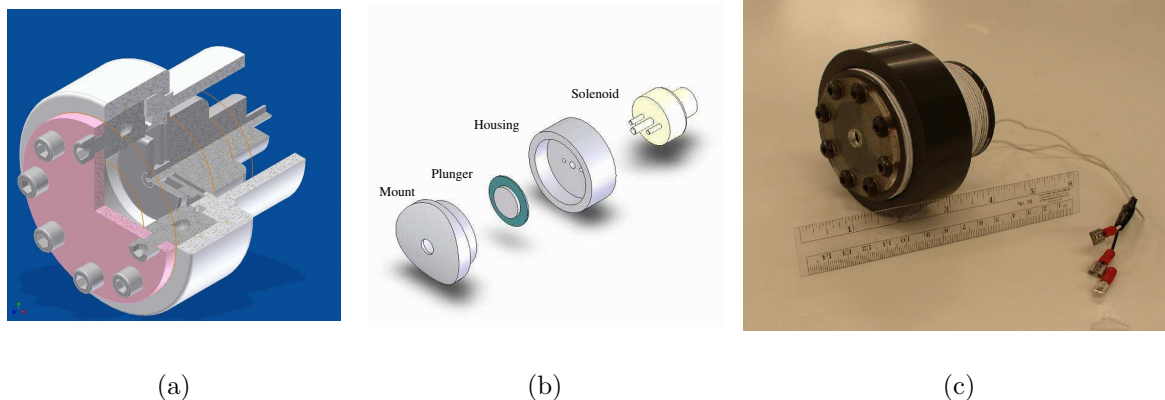


Figure 5: First generation of synthetic jet prototype [5; 20]: (a) CAD model of the actuator design. (b) Plunger and solenoid assembly. (c) Actual fabrication of the synthetic jet actuator.

Figure 5 shows the structure and appearance of a pulsatile jet actuator prototype [5; 20]. The driving diaphragms consist of a rigid disk with a flexible surround. Currently a solenoid actuator is used to generate the diaphragm motion. The fluid pushed by the moving diaphragm exits through an orifice. The experimental prototypes also allows easy substitution of different sized orifices and different sized chambers. In this way, physical parameters can be easily varied so that theoretical models (see below) can be compared against actual experimental results in different parameter regimes. This design has many advantages including its simplicity, very few moving parts, compactness, and no high tolerance (and therefore costly) components.

In order to quantify thrust generation we have designed and build a new synthetic jet actuator that

will give us the ability to change many design parameters. These includes, actuation frequency and amplitude, diaphragm velocity profile, cavity geometry, etc. The new prototype is shown in Figure 6. In the current design, the motion of the diaphragm, the frequency and amplitude of actuations, the exit diameter and the height and diameter of the cavity can be easily controlled. A cam mechanism is used to convert rotary motion into pre-defined reciprocating motion. We are in the process of direct measurement of force in this design.

COLORADO UNDERWATER VEHICLE TEST BEDS

Special design of UUVs are required in order to implement, demonstrate, and evaluate fully maneuverable self-contained hybrid underwater vehicles that

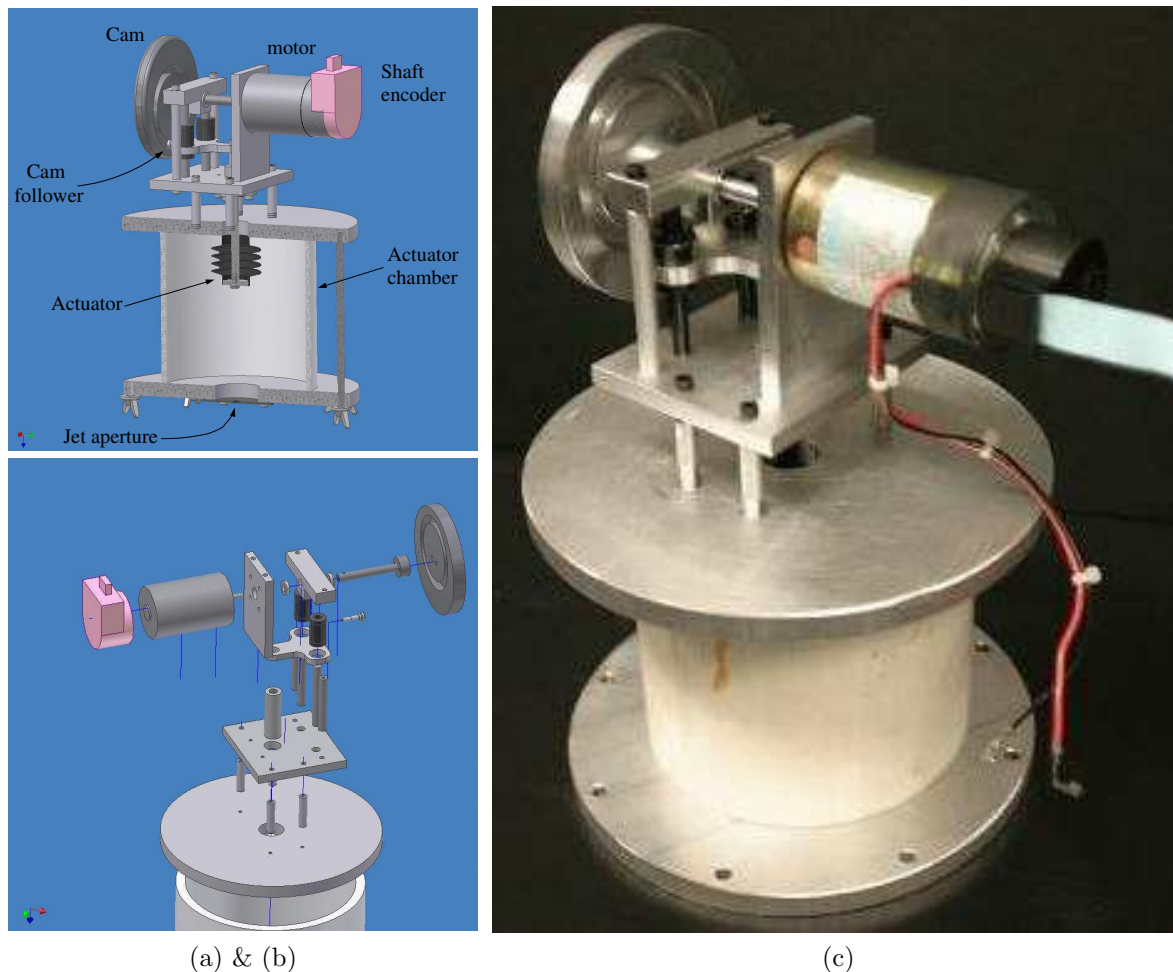


Figure 6: Second generation of synthetic jet prototypes capable of changing many actuation parameters (a) CAD model of the actuator design. (b) Actuator assembly. (c) Actual fabrication of the synthetic jet actuator.

combines pulsatile jet actuators with propeller-based propulsion schemes. To this end, the first phase of designing, building, and testing a Remote Controlled (RC) underwater vehicle, HydroBuff (see figure 7), was completed in early 2003 [6]. The first version of the HydroBuff is 1.4 m long, uses a conventional propeller and control surfaces, and is remotely controlled up to 5 ft depth. Below this depth, communication with the vehicle is not reliable. The vehicle is designed with 1% positive buoyancy, so in case of communication loss, the vehicle comes up to the surface.

A new lighter and shorter (around 1 m) underwater vehicle was recently designed and built at the University of Colorado at Boulder [5]. The new vehicle, Remote Aquatic Vehicle (RAV), can house up to four SJAs within the vehicle body, and will have an active buoyancy system (see Figure 7). RAV will

be used as a platform for testing the performance of the SJAs for low speed turning capabilities and high speed drag reduction. RAV is also designed with an expandable payload section capable of carrying various sensors for telemetry. This vehicle will serve as a model test-bed for hybrid vehicle designs that combine pulsatile jets with conventional propellers and torpedo-like bodies.

ANALYSIS OF SYNTHETIC JET ACTUATORS

The input design parameter for low speed maneuvering of UUVs is the revolution per minute (RPM) turn rate requirement or equivalently the angular velocity ω . From the required RPM one can calculate the drag moment experienced by the vehicle. We estimate the drag forces experienced by a submerged tube (see Figure 8) in rotation around an axis normal to its symmetry line. Since a differential element



Figure 7: UUV test beds at the University of Colorado. (Top) HydroBuff: A remotely controlled unmanned underwater vehicle [6]. (Bottom) RAV: An RC UUV capable of housing 4 pulsatile jet actuators [5].



(a)



(b)

Figure 8: Test of the synthetic jet actuator [20]. (a) Using SJAs to rotate a 4 inch diameter tube. (b) installation of SJAs on an 8 inch diameter tube, illustrating minimal impact of actuator on hull design.

of the tube at a radial distance of r away from the rotation axis has a local velocity of $V = r\omega$, which increases with distance from the rotation axis, the differential elements experience different drag forces. These forces can be estimated from drag data for flow behind a cylinder with diameter D at the local Reynolds number $Re = (r\omega)D/\nu$. Note that three dimensional, cross-flow, and flow-vehicle interaction effects are ignored in this simplified analysis. The total drag moment of a tube of length L rotating with an angular velocity of ω around its middle can be approximated by (ignoring external flow effects)

$$M_{\text{drag}} = 2 \int_0^{L/2} \frac{1}{2} \rho (r\omega)^2 C_D D r dr$$

or by changing the integration variable to the local Reynolds number Re

$$M_{\text{drag}} = \rho \frac{\nu^4}{\omega^2 D^3} \int_0^{Re_{L/2}} Re^3 C_D(Re) dRe \quad (1)$$

where C_D is the drag coefficient behind a cylinder at the local Reynolds number. The SJAs are expected to provide at least equal moment on the vehicle to overcome the drag moment.

In order to estimate the SJA moment we use the *slug model* (see *e.g.*, [17]) to approximate the thrust or impulse during the jet expulsion from the Helmholtz cavity. We assume the optimal formation number of $L_s/d \approx 4$ [15; 16; 17; 18; 21] for the ejecting slug of fluid with length L_s and the jet exit diameter d . Since water is incompressible, the

volume of the ejected jet (see figure 9b)

$$V_s = \frac{\pi d^2}{4} L_s$$

is equal to the volume displacement of the Helmholtz cavity due to the displacement of the diaphragm

$$V_D = \frac{\pi h}{8} (D_{ca}^2 + D_{cy}^2),$$

where h is the plunger stroke and D_{ca} and D_{cy} are the diameter of the cavity and the plunger, respectively. Consequently, the exit diameter (assuming $L_s/d \approx 4$) is related to the stroke length of the plunger (or diaphragm) through

$$\frac{L_s}{h} = \frac{D_{ca}^2 + D_{cy}^2}{2d^2}$$

Therefore, for optimal vortex formation, assuming $L_s/d \approx 4$

$$d^3 = \frac{h}{8} (D_{ca}^2 + D_{cy}^2) \quad \text{or} \quad L_s^3 = 8h (D_{ca}^2 + D_{cy}^2).$$

By knowing the stroke length of the plunger and its frequency one can easily estimate the generated impulse from the slug model to be $\rho\pi D^2 L_s U_j/4$, where ρ is the fluid density and $U_j = 2L_s f$ is the exiting jet velocity (proportional to the plunger velocity) during the expulsion period. An estimate of the moment of SJAs can be easily obtained by multiplying the SJA force with its moment arm. For a pair of actuators with a separation distance of l the net moment M_{SJA} can be estimated to be

$$M_{SJA} = 16\pi\rho D^4 f^2 l. \quad (2)$$

Results of these calculation for the 4.5 inch test tube shown in figure 8(b) are reported in figure 9(b). In order to accommodate for the reverse momentum during the ingestion part of the actuation a momentum adjustment factor of two is used. This is justified based on the calculations reported by Mittal *et al.* [22]. Calculated momentum drag in equation (1) is also shown in the Figure. The part of the SJA moment curves above the drag moment value represents enough actuation moment to overcome the drag. Figure 9(b) shows that the required drag moment can be overcome with various actuator exit diameters consistent with the optimal formation number of 4. Therefore, for a given solenoid stroke, one can estimate the optimal length of the ejected fluid, exit diameter, and attainable rotation rate of the submerged tube. Similarly the velocity

of the solenoid actuation (or its frequency) can be related to the jet velocity at the exit of the cavity. Consequently, for a given cavity geometry, exit diameter, solenoid actuation frequency, and solenoid stroke, one can calculate the SJA moment. This is also depicted in figure 9(b) as a function of the actuation frequency for various exit diameters.

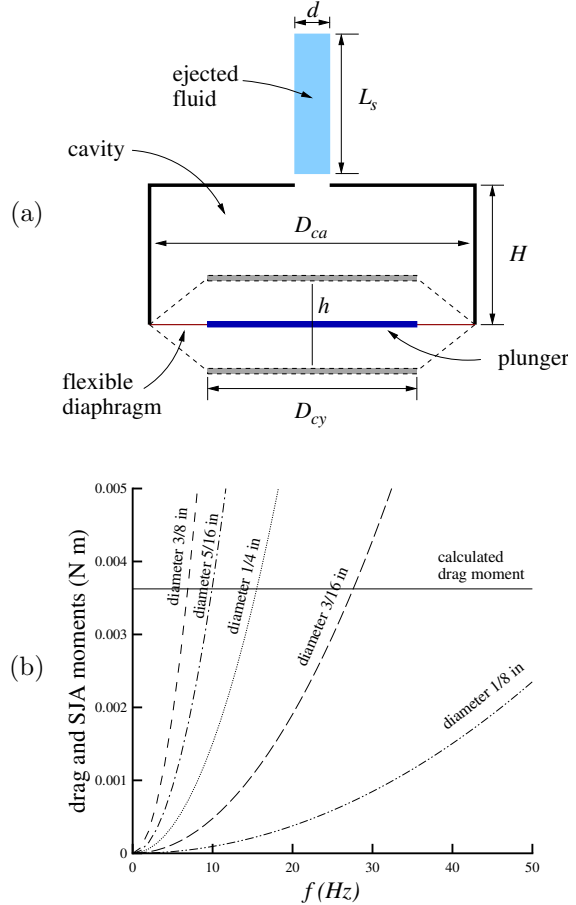


Figure 9: (a) Actuation of a synthetic jet actuator. (b) Thrusting moment vs. actuation frequency for various exit diameter at one rpm.

Larger exit diameters require less actuation frequency, and higher solenoid force for the specified duty cycle. The ability of the SJAs to rotate a submerged tube was demonstrated as depicted in Figure 8 in order to validate the models presented in this section. Our test results closely matched the hydrodynamic thrust model of Figure 9. More detailed account of the effect of various actuation parameters (d , D_{ca} , D_{cy} , f , and exit hole length, cavity and exit hole geometry) is the subject of a future publication.

CONCLUSIONS

Compact zero-mass pulsatile jets are proposed for low speed maneuvering of small underwater vehicles without sacrificing the common low drag body-of-revolution design. The actuation mechanism is simple, has very few moving parts, has no protruding components that increase drag, and takes up relatively little volume. Impulse extremization of vortex ring formation during impulsive ejection of fluid through the orifice of the actuators was investigated. The most relevant parameters in the design of the actuators are the plunger stroke and diameter, cavity diameter, jet exit diameter, and actuation frequency. The pinched-off state of an impulsive jet not only characterizes the energy extremization but also the extremum impulse state during the vortex ring formation. The same actuation mechanism could be used for flow control and drag reduction at higher cruising speeds. Progress on fabrication of actuators and their implementation in a small underwater vehicle are also reported.

ACKNOWLEDGMENT

The underwater vehicles in Figure 7 were designed as part of senior projects supervised by K. Mohseni and S. Palo in academic years 2002-2003 and 2003-2004. The author would like to acknowledge the help of involved students: M. Baumann, W. Dalbec, E. DeKruif, I. Morikawa, J. Novick, M. Rhodes and M. Schade for the HydroBuff [6] and M. Allgeier, K. DiFalco, D. Hunt, D. Maestas, S. Nauman, J. Poon, and A. Shileikis for the RAV [5]. The actuator in Figure 8(c) was designed as part of a summer independent study under the supervision of K. Mohseni by L. Copperberg, L. Georgieva, C. Madsen, L. McCrann, and E. Thomas [20]. The actuator in Figure 6 was designed during the summer of 2004 through an independent study by C. Madsen, S. Delanda and D. Maestas under K. Mohseni's supervision. The author would like to thank S. Palo for his contribution in the development of Colorado UUVs.

REFERENCES

- [1] J.G. Bellingham, C.A. Goudey, T.R. Consi, J.W. Bales, D.K. Atwood, J.J. Leonard, and C. Chryssostomidis. A second generation survey AUV. In *Proceedings of the 1994 Symposium on Autonomous Underwater Vehicle Technology*, pages 148–156, Cambridge, Massachusetts, June 1994.
- [2] D. Yoerger, J. Newman, and J.-J. Slotine. Supervisory control system for the Jason ROV. *IEEE Journal of Oceanic Engineering*, 11(3):392–400, 1986.
- [3] D.R. Yoerger, A.M. Bradley, and B.B. Walden et al. Surveying a subsea lava flow using the autonomous benthic explorer (abe). *Int. J. Syst. Sci.*, 29(10):1031–1044, 1998.
- [4] H.H. Wang, R.L. Marks, T.W. McLain, S.D. Fleischer, D.W. Miles, G.A. Sapilewski, and S.M. Rock. Otter: A testbed submersible for robotics research. In *ANS 1995*, 1995.
- [5] M. Allgeier, K. DiFalco, D. Hunt, D. Maestas, S. Nauman, J. Poon, supervised by K. Mohseni, A. Shileikis, and S. Palo. Senior design project: Remote Aquatic Vehicle. April 2004.
- [6] M. Baumann, W. Dalbec, E. DeKruif, I. Morikawa, J. Novick, M. Rhodes, supervised by K. Mohseni, M. Schade, and S. Palo. Senior design project: Hydrobuff R5L unmanned underwater vehicle. April 2003.
- [7] M. Nixon and J.B. Messenger, editors. *The Biology of Cephalopods*. Academic press, London, 1977.
- [8] R.K. O'Dor and D.M. Webber. The constraints on cephalopods: Why squid aren't fish. *Canadian Journal of Zoology*, 64:1591–1605, 1986.
- [9] R.K. O'Dor and D.M. Webber. Invertebrate athletes: Trade-offs between transport efficiency and power density in cephalopod evolution. *Journal of Experimental Biology*, 160:93–112, 1991.
- [10] J. Seikman. On a pulsating jet from the end of a tube, with application to the propulsion of aquatic animals. *J. Fluid Mech*, 15:399–418, 1963.
- [11] E.R. Trueman. Motor performance of some cephalopods. *Journal of Experimental Biology*, 49:495–505, 1968.
- [12] D. Weihs. Periodic jet propulsion of aquatic creatures. In W. Nachtigal, editor, *Bewegungsphysiologie – Biomechanik*, pages 171–175. 1977.
- [13] E. DeMont and J. Gosline. Mechanics of jet propulsion in the hydromedusan jellyfish, *Physalia physalis*. *Journal of Experimental Biology*, 134:347–361, 1988.

- [14] P.S. Krueger and M. Gharib. The significance of vortex ring formation to the impulse and thrust of a starting jet. *Phys. Fluids*, 15(5):1271–1281, 2003.
- [15] M. Gharib, E. Rambod, and K. Shariff. A universal time scale for vortex ring formation. *J. Fluid Mech*, 360:121–140, 1998.
- [16] K. Mohseni, H. Ran, and T. Colonius. Numerical experiments on vortex ring formation. *J. Fluid Mech*, 430:267–282, 2001.
- [17] K. Mohseni and M. Gharib. A model for universal time scale of vortex ring formation. *Phys. Fluids*, 10(10):2436–2438, 1998.
- [18] K. Mohseni. Statistical equilibrium theory of axisymmetric flows: Kelvin’s variational principle and an explanation for the vortex ring pinch-off process. *Phys. Fluids*, 13(7):1924–1931, 2001.
- [19] K. Mohseni. Studies of two-dimensional vortex streets. AIAA paper 2001-2842, June 2001. 31st AIAA Fluid Dynamics Conference and Exhibit, Anaheim, CA.
- [20] L. Copperberg, L. Georgieva, C. Madsen, L. McCrann, and supervised by K. Mohseni E. Thomas. Summer project: Zero-mass change synthetic submarine maneuvering jets. August 2003.
- [21] K. Mohseni. Impulse extremization in vortex ring formation. *Discrete and Continuous Dynamical Systems – Series B*, pages Invited paper, to appear, 2003.
- [22] R. Mittal, P. Rampunggoon, and H. S. Udaykumar. Interaction of a synthetic jet with a flat plate boundary layer. AIAA paper 2001-2773, 2001.